Report for the Australian and New Zealand Head and Neck Cancer Society Foundation Grant 2025 (Adenoid Cystic Carcinoma fund)

Principal Investigator: Dr Rajdeep Chakraborty (BDS, MSc, MRes, PhD)
School of Natural Sciences, Faculty of Science and Engineering, Macquarie University

Title: Functionalised nanoparticles transforming adenoid cystic carcinoma into an immune hot tumour

Background: Treatment options for surgically inoperable or metastatic salivary gland cancer are restricted to chemotherapy. To date immunotherapy that includes immune check point inhibitors like Pembrolizumab and Nivolumab are not approved by FDA for the management of salivary gland cancer [1]. KEYNOTE-028 (NCT02054806) showed objective response rate of 12% with a 4-month median duration of response [1] and overall response rate of nivolumab was 4% [2]. Mucoepidermoid carcinoma (MEC) exhibit immune-hot tumour microenvironment (TME), whereas adenoid cystic carcinoma (ACC) shows contrasting features of immune-cold TME [3]. Objective response rate of immune check point inhibitors depends on the expression of PD-1 expression [3]. MEC express PD-1, showed an impressive objective response rate of approximately 33%, whereas ACC show negative PD-1 expression, presented a poor response rate of approximately 4-8% [3].

Immunological subtyping of salivary gland cancer identified variation of several pathways that includes apoptotic pathway in adenoid cystic carcinoma and mucoepidermoid carcinoma that might impact immunotherapy, due to diverse intrinsic cell compositions based on histologic origin [4]. So far, apoptosis has been found to tune tumour immunity based on the demonstration of apoptosis of immune cells (T effector cells), that undermines the anti-tumour reactivity of immune cells in the TME. This eventually facilitates the growth of T regulatory cells, M2 macrophage, and myeloid derived suppressor cells [5].

We previously found high expression of immunosuppressive proteins in salivary gland cancer cells that might be responsible for the lowering of immunotherapy efficacy [6]. Thus, based on the previous findings, we initially performed 3D-salivary gland – immune co-culture model construction and discovery phase mass spectrometry. We found significant low protein expression of Annexin A3 (ANXA3) in ACC compared to MEC cell lines. ANXA3 promotes immune infiltration and improves tumour prognosis [7], this might be one of the possible reasons for MEC exhibiting an immune-hot TME, whereas ACC shows features of immune-cold TME [3].

We, therefore, hypothesized that overexpression of Annexin A3 using functionalized nanoparticle will transform ACC into an immune hot tumour. To substantiate the hypothesis, we functionalized both gold nanoparticles (as a proof-of-concept) and PLGA nanoparticles (FDA approved) with anti-cMyb antibody. We did biophysical chemistry and *in vitro* characterization of the functionalized nanoparticles. After determining successful immobilization or conjugation of anti-cMyb antibody onto nanoparticles, we overexpressed Annexin A3 by conjugating recombinant ANXA3 onto anti-cMyb antibody functionalized PLGA nanoparticles. We determined the successful conjugation of recombinant ANXA3 protein using western blot and confocal microscope images. We overexpressed ANXA3 in ACC spheroids in PBMC coculture model and determined immune infiltration and size of the spheroids.

Results:

Overexpression of ANXA3 protein

To substantiate our hypothesis, next, streptavidin coated PLGA nanoparticles were conjugated with biotinylated [Alexa Fluor 647 labelled anti-MYB antibody and recombinant ANXA3 protein (1:1)], and added to ACC cells to overexpress ANXA3 and assess immune infiltration in the 3D cell culture matrix. 3D z stack imaging confirmed significant amount of positive far-red Alexa Fluor 647 bright opaque fluorescent specs signifying successful uptake of ANXA3 conjugated anti-cMyb antibody functionalized PLGA nanoparticles in UM-HACC-2A and UFH2 cells. Whereas, upon addition of Alexa Fluor 647 labelled streptavidin PLGA nanoparticles did not show significantly observable fluorescence specs. Here, Alexa Fluor 647 labelled streptavidin PLGA nanoparticles acted as a negative control. Western blot analysis done to further confirm successful uptake of ANXA3 conjugated anti-cMyb antibody functionalized PLGA nanoparticles. ANXA3 Recombinant Protein acted as positive control, PLGA acted as negative control, UM-HACC-2A, UFH2 acted as experimental control, and GAPDH as internal control of the experiment. Western blot further confirmed successful uptake of ANXA3 conjugated anti-cMyb antibody functionalized PLGA nanoparticles in ACC cells, showing significant increase of ANXA3 protein (35 kDa) after using functionalized nanoparticles (Figure 1).

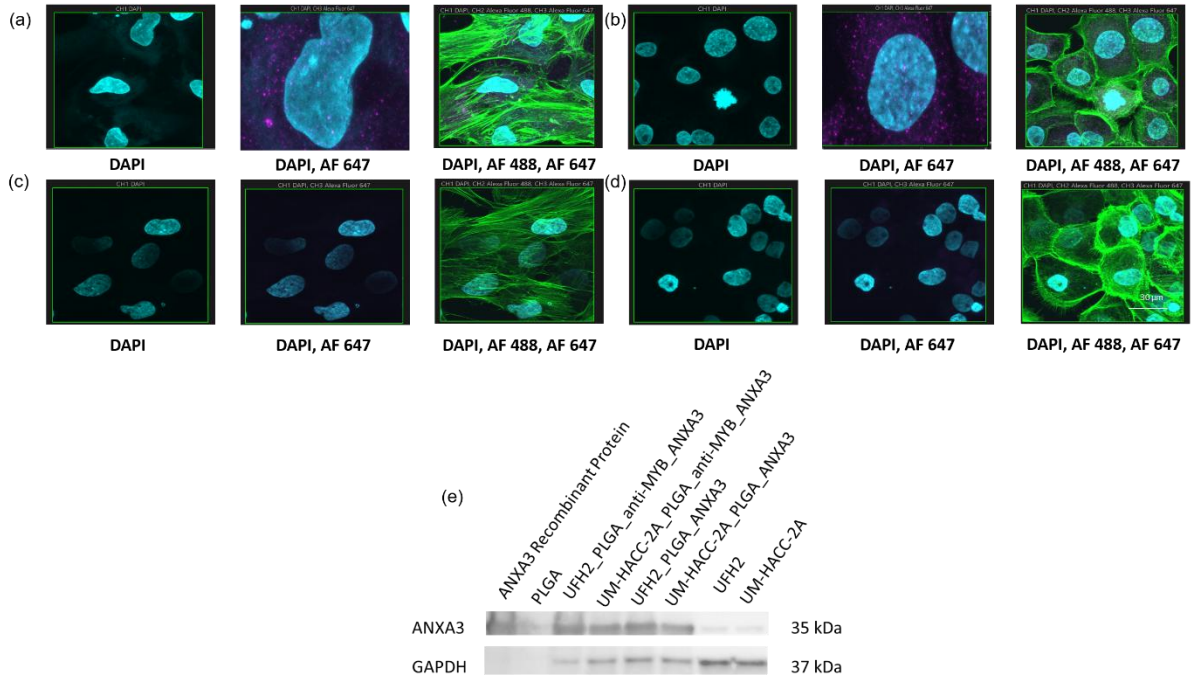


Figure 1 Functionalization of anti-cMyb antibody-PLGA nanoparticles with recombinant ANXA3 protein. Alexa Fluor 647 was conjugated to the biotinylated mixture using Alexa Fluor 647 conjugation kit (Fast) – Lightening Link (AB269823-1004, abcam). 3D z-stack confocal images with 60X objective of (a) anti-cMyb antibody-ANXA3-PLGA nanoparticles on UM-HACC-2A cells; (b) anti-cMyb antibody-ANXA3-PLGA nanoparticles on UFH2 cells; (c) Alexa Fluor 647-PLGA nanoparticles on UM-HACC-2A cells; (d) Alexa Fluor 647-PLGA nanoparticles on UFH2 cells; Scale 30 µm; (e) western blot showing overexpression of ANXA3 using anti-cMyb antibody-ANXA3-PLGA nanoparticles. UM-HACC 2A and UFH2 acted as a control, ANXA3 recombinant protein acted as a positive control and PLGA acted as a negative control. Positive control 4 µg, control 10 µg, and the rest of the samples 8 µg was loaded. Pre-stained protein ladder (ab116029, abcam), Rabbit annexin A3 polyclonal antibody (PA5-82483, Thermo Fisher Scientific) at 0.4 µg/mL, Goat anti-Rabbit IgG (H+L) Secondary Antibody, HRP (31460, Thermo Fisher Scientific) at 1:10,000, mouse GAPDH monoclonal

antibody ZG003 (398600, Thermo Fisher Scientific) at 2 µg/mL, and Goat anti mouse IgG HRP (31430, Thermo Fisher Scientific) at 1:5000.

Overexpression of ANXA3 protein resulted in increased immune infiltration and reduction of the shape of the ACC spheroids

Upon addition of ANXA3 conjugated anti-cMyb antibody functionalized PLGA nanoparticles to UM-HACC-2A and UFH2 spheroids on 3D ECM in a PBMC coculture model resulted in significant increase of CD4+ and CD8+ positive lymphocytes in the ECM incrementally over time, that is, at 72 hours showed maximum infiltration of tumour infiltrating lymphocytes (Figure 2). The control groups UM-HACC-2A and UFH2 spheroids on 3D ECM in a PBMC coculture did not show much variation in CD4+ and CD8+ positive lymphocytes over time (Figure 8). Recombinant GAPDH protein (non-specific control) overexpression following similar protocol was done. The non-specific control did not result in significant change in CD4+ and CD8+ positive lymphocytes in ECM over time (Figure 3).

Ostensibly, the UM-HACC-2A and UFH2 spheroids showed significant reduction in size upon addition of ANXA3 conjugated anti-cMyb antibody functionalized PLGA nanoparticles in the PBMC coculture model compared to the control groups (Figure 4).

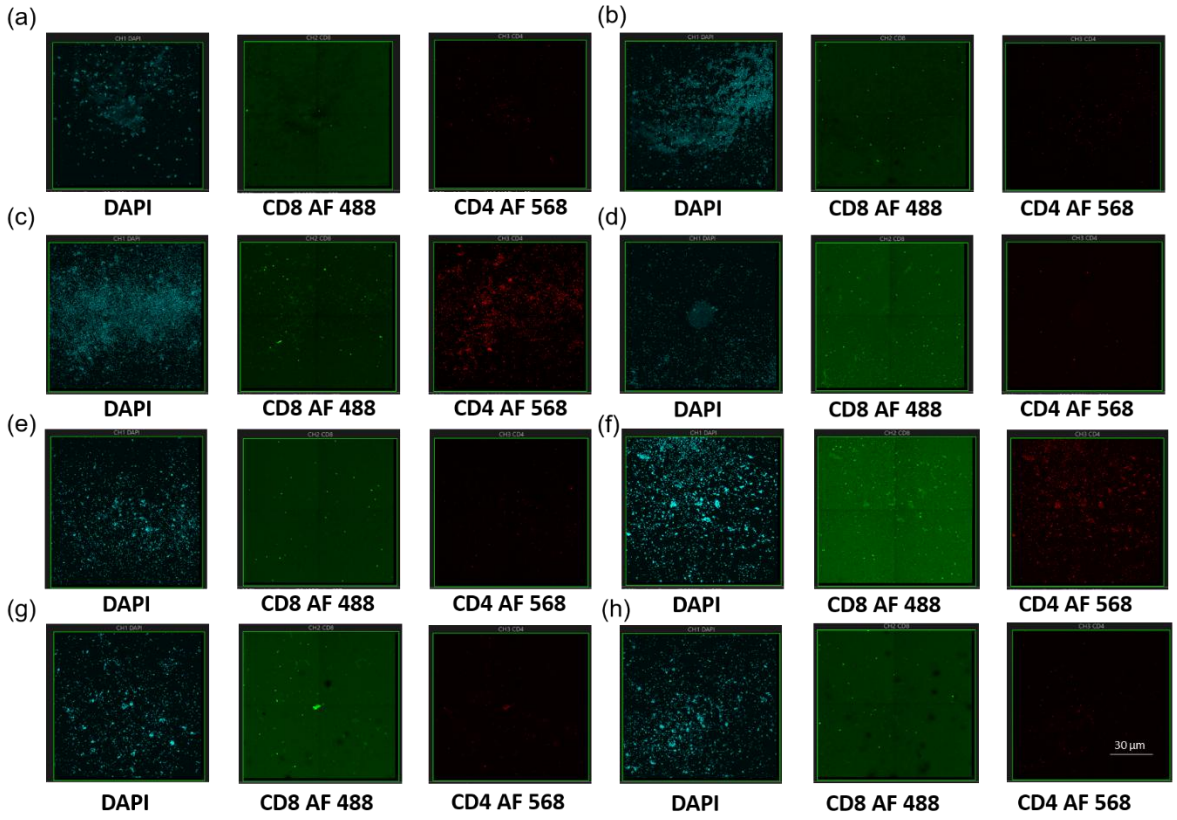


Figure 2 Infiltration of immune cells in ACC TME due to ANXA3. 3D z-stack confocal images of CD4+ and CD8+ with 60X objective of (a) anti-cMyb antibody-ANXA3-PLGA nanoparticles on UM-HACC-2A spheroids in PBMC coculture in 24 hours; (b) anti-cMyb antibody-ANXA3-PLGA nanoparticles on UM-HACC-2A spheroids in PBMC coculture in 48 hours; (c) anti-cMyb antibody-ANXA3-PLGA nanoparticles on UM-HACC-2A spheroids in PBMC coculture in 72 hours; (d) anti-cMyb antibody-ANXA3-PLGA nanoparticles on UFH2 spheroids in PBMC coculture in 24 hours; (e) anti-cMyb antibody-ANXA3-PLGA nanoparticles on UFH2 spheroids in PBMC coculture in 48 hours; (f) anti-cMyb antibody-ANXA3-PLGA nanoparticles on UFH2 spheroids in PBMC coculture in 72 hours; (g) anti-cMyb antibody-

GAPDH-PLGA nanoparticles on UM-HACC-2A spheroids in PBMC coculture in 72 hours; (h) anti-cMyb antibody-GAPDH-PLGA nanoparticles on UFH2 spheroids in PBMC coculture in 72 hours. Scale 30 µm.

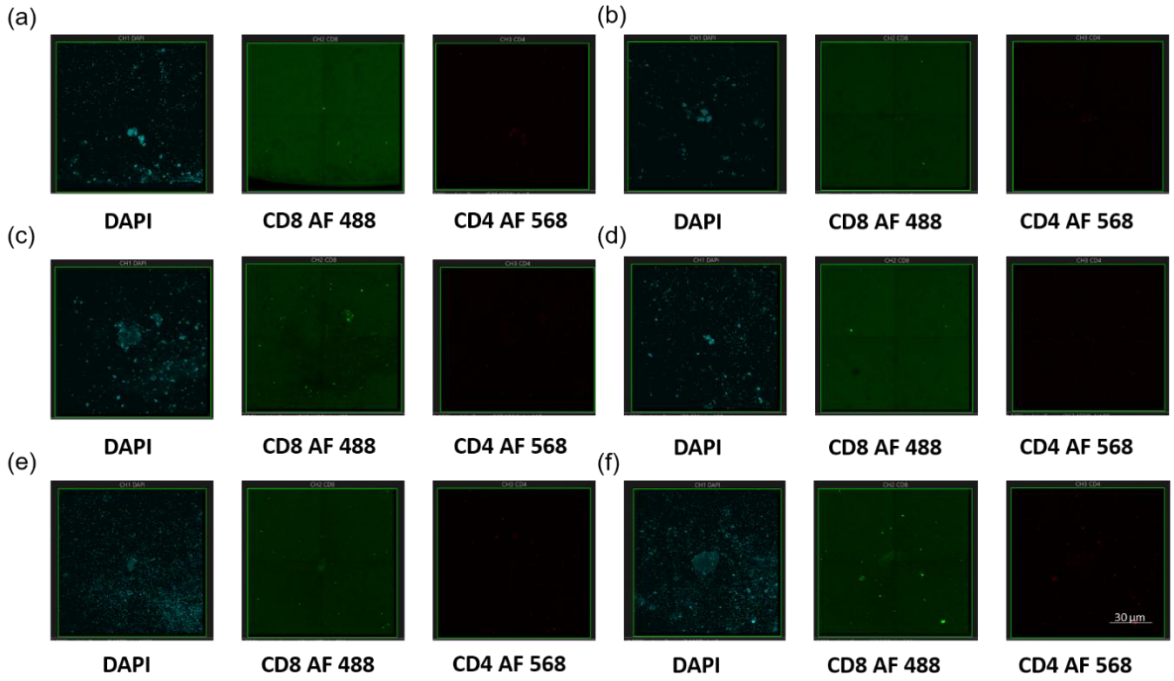


Figure 3 Infiltration of immune cells in ACC TME. 3D z-stack confocal images of CD4+ and CD8+ with 60X objective of (a) UM-HACC-2A spheroids in PBMC coculture in 24 hours; (b) UM-HACC-2A spheroids in PBMC coculture in 48 hours; (c) UM-HACC-2A spheroids in PBMC coculture in 72 hours; (d) UFH2 spheroids in PBMC coculture in 24 hours; (e) UFH2 spheroids in PBMC coculture in 48 hours; (f) UFH2 spheroids in PBMC coculture in 72 hours. Scale 30 µm.

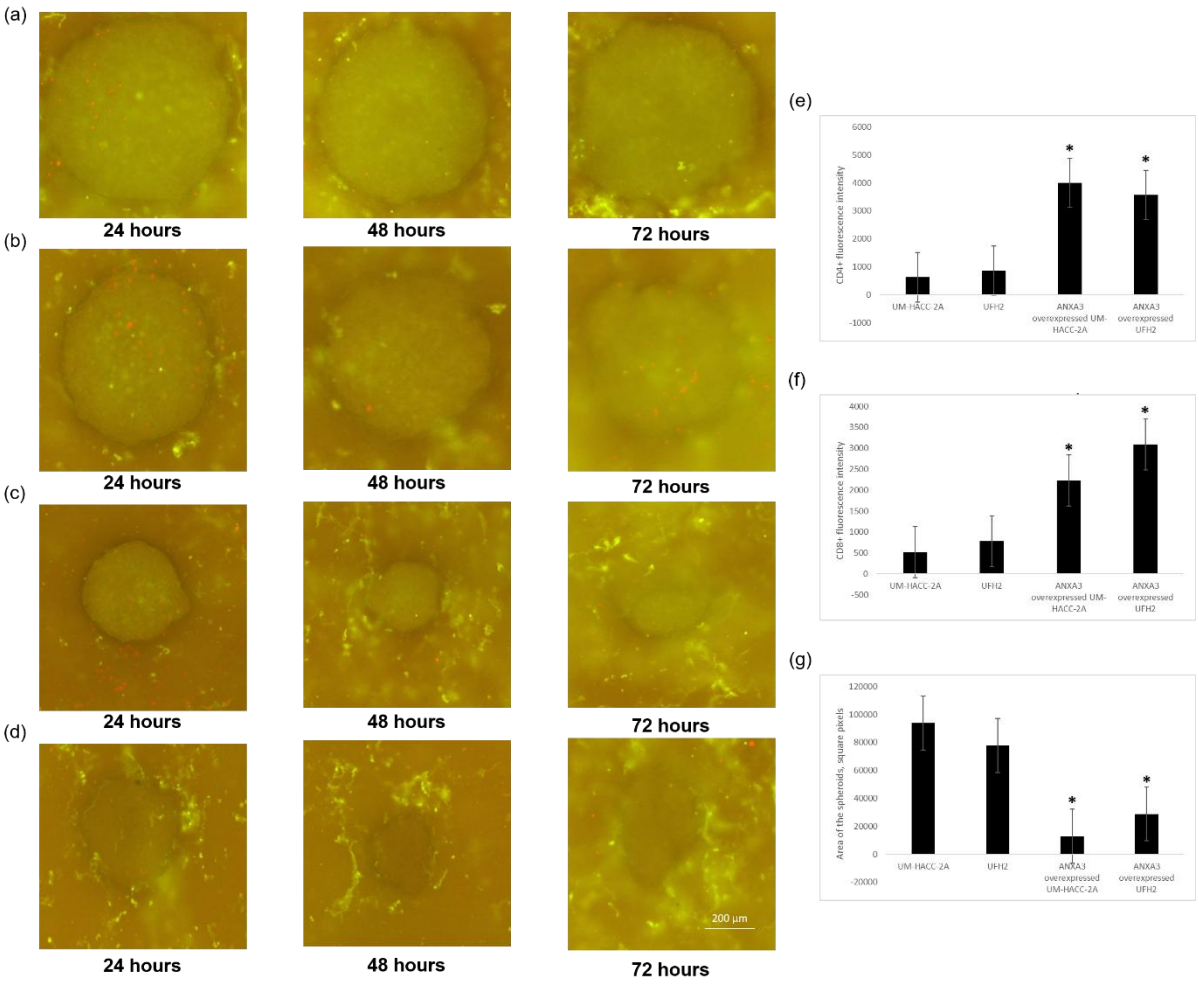


Figure 4 Effect of immune cells infiltration on ACC spheroids due to ANXA3. Widefield microscope images with 4X objective of (a) UM-HACC-2A spheroids in PBMC coculture; (b) UFH2 spheroids in PBMC coculture; (c) anti-cMyb antibody-ANXA3-PLGA nanoparticles on UM-HACC-2A spheroids in PBMC coculture; (d) anti-cMyb antibody-ANXA3-PLGA nanoparticles on UFH2 spheroids in PBMC coculture. Scale 200 µm. Bar graphs showing (e) CD4+ fluorescence intensity, (f) CD8+ fluorescence intensity, and (g) area of the spheroids of UM-HACC-2A spheroids in PBMC coculture, UFH2 spheroids in PBMC coculture, anti-cMyb antibody-ANXA3-PLGA nanoparticles on UM-HACC-2A spheroids in PBMC coculture, and anti-cMyb antibody-ANXA3-PLGA nanoparticles on UFH2 spheroids in PBMC coculture respectively (n=6); *$P \leq 0.05$. The error bar represents standard error of the mean.

Overexpression of ANXA3 protein resulted in variation in apoprotic proteins

Upon apoptotic profiler result analysis, Pro caspase 3 and cleaved caspase 3 expressions were found significantly higher in adenoid cystic carcinoma spheroids treated with ANXA3 conjugated anti-cMyb antibody functionalized PLGA nanoparticles (Figure 5). Additionally, HSP27, SMAC, and catalase are significantly high in functionalized nanoparticle treated ACC spheroids to untreated (Figure 5). Ostensibly, survivin are significantly lower in ANXA3 overexpressed ACC spheroids. Fas-Associated Death Domain (FADD) is significantly lower in the same compared to the control (Figure 5). Interestingly, Bad, Bcl x, HIF 1 alpha, HSP60, and HSP70 showed variation in expression changes in UM-HACC-2A and UFH2 spheroids after ANXA3 overexpression (Figure 5).

p53 at position serine 392, 46, and 15 expressions are significantly high in ANXA3 overexpressed ACC spheroids (Figure 5). Similarly, PON2, TRAIL R1 or DR4, p21 or CIP1, TRAIL R2 or DR5, Bax, p27 or Kip1, Bcl 2, Fas or CD95, HO 1 or HSP32, Rad17 S635, HO 2 or HMOX2, cIAP 1, cIAP 2, TNF R1, Claspin, XIAP, HTRA2 or Omi, Clusterin, Livin, and Cytochrome c showed significant higher expressions in ANXA3 overexpressed ACC spheroids (Figure 5).

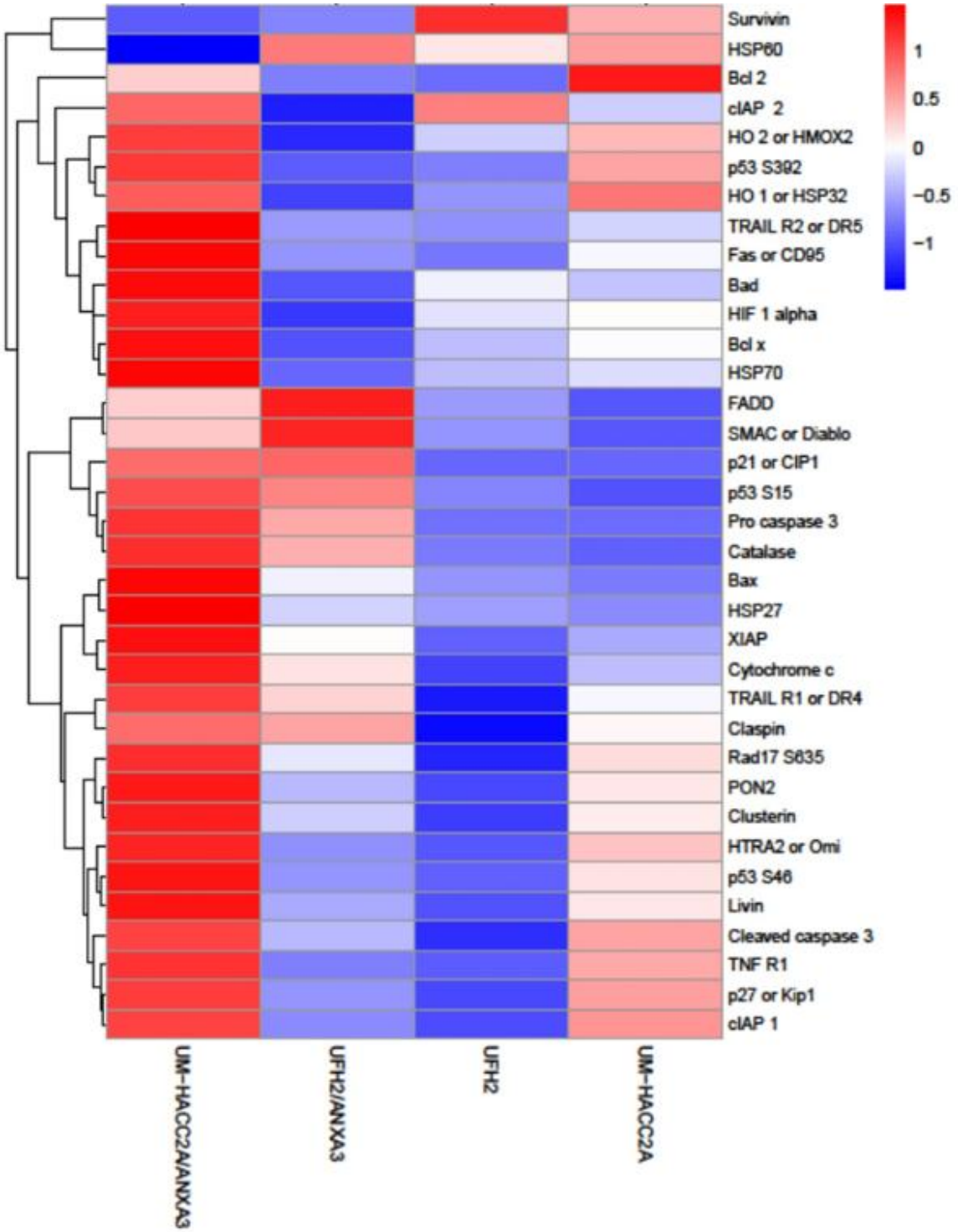


Figure 5 Differential apoptotic proteins due to the effect of immune infiltration induced by ANXA3 in ACC spheroids. Comparison of apoptotic protein expressions in UFH2 in PBMC coculture, UM-HACC-2A in PBMC coculture, anti-cMyb antibody-ANXA3-PLGA nanoparticles on UM-HACC-2A spheroids in PBMC coculture, and anti-cMyb antibody-

ANXA3-PLGA nanoparticles on UFH2 spheroids in PBMC coculture. Heat map to visualize hierarchical clustering of apoptotic proteins in A-253 and ACC cells in 3D immune co-culture model made with heatmap.2() [gplots R package]. The protein intensities are log10 transformed and are displayed as colours ranging from blue to red as shown in the key. Both rows and columns are clustered using correlation distance and average linkage.

Conclusion: Overall, this project shows a promising approach to transform ACC into an immune "hot" tumour. In future, ANXA3 functionalized nanoparticles should be tested *in vivo*.

References:

[1] Cohen RB, Delord JP, Doi T, Piha-Paul SA, Liu SV, Gilbert J, Algazi AP, Damian S, Hong RL, Le Tourneau C, Day D, Varga A, Elez E, Wallmark J, Saraf S, Thanigaimani P, Cheng J, Keam B. Pembrolizumab for the Treatment of Advanced Salivary Gland Carcinoma: Findings of the Phase 1b KEYNOTE-028 Study. Am J Clin Oncol. 2018 Nov;41(11):1083-1088.

[2] Niwa K, Kawakita D, Nagao T, Takahashi H, Saotome T, Okazaki M, Yamazaki K, Okamoto I, Hirai H, Saigusa N, Fushimi C, Masubuchi T, Miura K, Okazaki SI, Matsui H, Okada T, Iwaki S, Matsuki T, Hanyu K, Tsukahara K, Oridate N, Tada Y. Multicentre, retrospective study of the efficacy and safety of nivolumab for recurrent and metastatic salivary gland carcinoma. Sci Rep. 2020 Oct 12;10(1):16988.

[3] Sato R, Yamaki H, Komatsuda H, Wakisaka R, Inoue T, Kumai T, Takahara M. Exploring Immunological Effects and Novel Immune Adjuvants in Immunotherapy for Salivary Gland Cancers. Cancers (Basel). 2024 Mar 19;16(6):1205.

[4] Hong J, Choi E, Kim D, Seo MK, Kang H, Park B, Kim S. Immunological subtyping of salivary gland cancer identifies histological origin-specific tumor immune microenvironment. NPJ Precis Oncol. 2024 Jan 20;8(1):15.

[5] Liu J, Hong M, Li Y, Chen D, Wu Y, Hu Y. Programmed Cell Death Tunes Tumor Immunity. Front Immunol. 2022 Mar 30; 13:847345.

[6] Chakraborty R., Darido C., Tay A., Zaw T., Ranganathan S., Liu F., & Palmisano G. Inhibition of anti-tumour reactivity of immune cells in the salivary gland cancer: a proteomic approach. Oral Oncology Reports. 2024; (100160)9: 1-9.

[7] Li DQ, Lin M, Abdelrahman Z. High expression of the ANXA3 gene promotes immune infiltration and improves tumor prognosis in ovarian serous carcinoma using bioinformatics analyses. Ann Transl Med. 2022 Oct;10(19):1055.